Research Article

Chemical Review and Letters
journal homepage: www.chemrevlett.com
ISSN (online): 2645-4947 (print) 2676-7279

Utilization of Nanoparticle Prepared from Local Nigerian Hen Egg Shell as an Adsorbent for the Removal of Methylene Blue dye from aqueous solution : DFT and Experimental Study

Paul Ocheje Ameh[1,] *

[1] *Physical Chemistry Unit, Department of Chemistry, Nigeria Police Academy, Wudil, P. M B. 3474, Kano State Nigeria*

ARTICLE INFO

Article history:
Received 11 February 2022
Received in revised form 18 March 2022
Accepted 26 January 2023
Available online 2 April 2023

Keywords:
Adsorption kinetics
Density function theory
Egg shell nanoparticles
Methylene blue Dye

ABSTRACT

Adsorption capacity of nanoparticle prepared from waste hen egg shell for the removal of methylene blue dye from aqueous solution was investigated using batch and density function theory (DFT) process. The prepared egg shell nano particle (PESNP) were characterized using proximate X-ray fluorescence, Scanning electron microscopy, (SEM) and Thermogravimetric analysis. The results obtained indicated that PESNP is a good adsorbent for methylene blue. Their adsorption capacity was found to be influenced by initial dye concentration, adsorbent dose, pH, temperature and by the period of contact. The adsorption of the dye onto PESNG was found to be physical, spontaneous and best described by Freundlich and Temkin adsorption models. Adsorption kinetic study indicated that a pseudo second order kinetics was favoured. Results from the quantum chemical study indicated that the adsorption of methylene blue onto PESNP will preferentially occur through the sulphonium sulphur, nitrogen and benzene ring as the highest Fukui functions were found to reside in those atoms

1. Introduction

The global population has grown significantly over the last few decades; this has led to a great increase in the demand for water supply. Access to potable water is becoming a luxury due to exploitation of the limited amount of freshwater in Earth's freshwater reserves [1 – 2]. One of the major problems concerning environmental pollutants is wastewater problem coming from both domestic and industry. Small and medium-sized enterprises (SMEs) are also major contributors to industrial wastewater pollution because of the lack of space and financial resources to install on-site treatment facilities. They often discharge bleaches, salts, organics, dyes etc. into water bodies without proper treatment. Some dyes which are one of the common water contaminants are non-biodegradable in nature, highly water-soluble, stable to light and oxidation. They have been found to be generally mutagenic, carcinogenic and can cause severe damages to human beings, such as dysfunction of the kidneys, reproductive system, liver and brain and central nervous system [3].

Many conventional methods such as precipitation, ion exchange, solvent extraction, adsorption, filtration, electrochemical treatment have been applied for removal of contaminants from industrial wastewaters. Adsorption using activated carbon has been reported to be one of the best known methods for the removal of contaminants from water [4]. In the literature, great attention has been given to sourcing cheaper, locally available and renewable materials as precursors for producing activated carbon with comparable functionalities to the commercial product [5 – 6]. Examples of agricultural wastes and byproducts that have been successfully used for waste water treatment include walnut shell [7], apple peels [8], almond shell [9], *Zizuphus jujuba* cores [10], date [11], rice husk [12], coconut shell [13], palm kernel shell [14], bamboo waste [15] and macadamia nutshell [16]. Some of the challenges associated with most adsorbents are inadequate surface area, thermal instability, influence of pH and solution physicochemical properties.

Nano materials have been widely reported as efficient adsorbents that have uplifted future hope in remediating water pollution [17]. Therefore, this research is designed to prepare nanoparticles from waste hen egg shell generated in Nigeria Police Academy Wudil Kano state

* Corresponding author.; e-mail: amehpaul99@gmail.com
https://doi.org/10.22034/crl.2023.328721.1155

Nigeria for the removal of methylene blue dye form aqueous solution. The hen eggshells are usually generated by cadets of the academy as waste in large quantities around the kitchen area causing unpleasant odours from biodegradation, damaging microbial activity and altering characteristics of the soil. Characterization of the synthesized egg shell nano particle (PESNP) was done using proximate X-ray fluorescence, Scanning electron microscopy, (SEM) and Thermogravimetric analysis. The capability of the nano materials upon adsorbing methylene blue dye molecules was quantified using batch equilibrium studies while computational chemistry study was applied to predict the feasibility and mechanism of adsorption of the studied dyes in the environment

2. Materials and methods

2.1. Materials

All reagents used for this experimental work were carefully selected and certified to be of analytical grade and prepared with distilled water. The glass wares were washed with liquid soap, rinsed with water, soaked in 10 % HNO_3 for 24 hours rinsed with deionised water. Waste hen eggshells were collected from the cafeteria of Nigeria Police Academy Wudil, Kano State Nigeria. The collected egg shell samples were cleaned following the method described by Kumaraswamy *et al* [18]. The cleaned eggshells were oven dried at 150°C for 3 hours to remove water. The dried substance was ground thoroughly in a mortar and sieved into 100 µm particle size. The obtained eggshell powder after sieving was thereafter kept in desiccators at a room temperature for further study.

2.2. Preparation of Egg Shell Nano particle (PESNP)

The egg shell nanoparticle (PESNP) was prepared through sol-gel method as described by Jalu *et al* [19]. The gel obtained was calcined in a muffle furnace under air atmosphere at 900 °C, for 1 hour. After calcining, the sample was cooled in air for 20 minutes to avoid the hydrolysis [20].

2.3. Proximate Analysis

The proximate analysis of the prepared egg shell nano particle was carried out as reported [21 – 23]. Analysis carried out included determination of pH, moisture, ash contents, bulk density and dry matter of PESNP.

2.4. Batch equilibrium studies

Batch experiments of adsorption were carried out in 250 cm^3 Erlenmeyer flasks where solutions of dye (100 mL) with different initial concentrations (10–100 mg/L) were placed. The original pH (6) of the solutions was used. Equal masses of 0.5 g of the adsorbent (PESNP) were added to the dye solutions, and the mixtures were then kept in a thermostatic shaker at 303 K for 80 minutes to reach equilibrium.

A similar procedure was followed for another set of Erlenmeyer flask containing the same dye concentration without adsorbent to be used as a blank. The flasks were then removed from the shaker, and the final concentration of dye measured at 630 nm, using UV–vis spectrophotometer (Jenway, Model 6405).

The amount of the dye adsorbed (q_e) and the percentage of dye removal (%Rem) were calculated using equation 1a and 1b respectively :

$$q_e = \frac{V(C_0 - C_e)}{1000} \quad (1a)$$

$$\%Rem = \frac{V(C_0 - C_e)\ x\ 100}{C_0} \quad (1b)$$

where q_e is the amount of dye adsorbed in milligram per gram of the adsorbent, C_0 and C_e (mg/L) are the liquid-phase concentrations of dye at initial and any time *t*, respectively; *V* the volume of the solution (L).

The effect of initial pH (2 – 12) on the adsorption of methylene blue dye by PESNP was studied at 0.5 g adsorbent, 100 mL of 100 mg/L of the dye and a temperature of 303 K. The pH of the solution was adjusted by adding a few drops of dilute 1.0 M NaOH or 1.0M HCl before each experiment.

To study the effect of temperature on the removal by PESNP, the experimental condition consisted: pH 6.0, 0.5 g adsorbent and initial dye concentration of 100 mg/L for 80 mins.

The effect of contact time and adsorbate dose were studied by keeping all other parameters constant and by varying the time and adsorption dose respectively, the adsorption experiment highlighted above was adopted and the percentage removal of the methylene blue adsorbed at different time and for different adsorption dose were respectively calculated.

2.5. Scanning electron microscopy (SEM) analysis

Scanning electron microscopy (SEM) analysis of PESNP before and after treatment with methylene blue dye was carried out using Scanning electron microscope, model number JSM- 5600 LV produced by JEOL, TOKYO, Japan at magnification of 10000 X in order to reveal their surface morphology. Scanned micrographs were taken at an accelerating voltage of 2.00 and 15.00 kV.

2.6. Thermal analysis

A differential scanning calorimeter (DSC, NETZSCH 409) and a simultaneous thermal analyzer (STA, NETZSCH 409) was used to evaluate the thermal properties of the prepared egg shell nano particle. The thermo gravimetric analysis – differential Scanning Calorimetry (TGA – DSC) curves was obtained with a heating rate of 50°C/min under nitrogen atmosphere within the temperature range of 50 – 600°C and DSC scanning range of 0 – 120 mcal/sec

2.7. X-ray Fluorescence Analysis

X-ray fluorescence (XRF) analysis of both the raw egg shell and the prepared egg shell nano particle was performed to ascertain their chemical composition using an X-ray fluorescence (XRF) (Philips, model PW 2400) at a tube current of 1000 A with an acquisition lifetime of 30 s. The XRF diffraction pattern was used to determine the percentages of chemical compositions

2.8. Quantum chemical parameters

Quantum-chemical calculations based on DFT were performed using DMol3 package contained in the Materials Studio 7.0 software (Accelrys, Inc.). All calculations were performed using B3LYP functional with ‘‘double-numeric plus polarization” (DNP) basis set in gas phase model [Ameh, 2018]. Koopman’s theorem was used to calculate the ionization energy (IP), electron affinity (EA), electrophilicity index (ω), nucleophilicity index (N) and other chemical reactivity descriptors which provide insights into chemical reactivity and selectivity, in terms of global parameters such as electronegativity (χ), hardness (η), and softness (σ), and local ones such as the Fukui function f(r) as shown below [24]:

$$IP = -E_{HOMO} \quad (2)$$

$$EA = -E_{LUMO} \quad (3)$$

$$\Delta E = E_{LUMO} - E_{HOMO} \quad (4)$$

$$\chi = \frac{E_{HOMO} + E_{LUMO}}{2} \quad (5)$$

$$\eta = \frac{E_{LUMO} - E_{HOMO}}{2} \quad (6)$$

$$\omega = \frac{\chi^2}{2\eta} \quad (7)$$

$$\sigma = \frac{1}{\eta} \quad (8)$$

$$N = E_{HOMO} - E_{HOMO(TCE)} \quad (9)$$

$$f_k^+ = q_k(N+1) - q_k(N) \quad (10)$$

$$F_k^- = q_k(N) - q_k(N-1) \quad (11)$$

3. Results and Discussion

3.1. Proximate analysis and Adsorbent Characterization

3.1.1. Proximate analysis

The results obtained from the proximate analysis of both the raw egg shell (RES) and the prepared egg shell nano particle (PESNP) is as presented in Table 1.

Table 1. Results from Proximate Analysis

S/N	Parameter	RAW EGG SHELL	PREPARED EGG SHELL NANOPARTICLE
1	pH of 1 % solution	6.20	6.43
2	Moisture content (%)	0.993	0.214
3	Ash content (%)	73.62	98.25
4	Dry matter (%)	25.41	1.54
5	Bulk density (g/cm^3)	0.678	0.989

The percentage moisture of RES and PESNP are 0.993 % and 0.214 % respectively. The moisture content of a sample usually refers to the water content of that sample. It has reported that the yield and quality of activated carbon is usually improved by the removal of moisture [25]. Hence it is expected that PESNP should be a better adsorbent than RES because of its low moisture content. The percent moisture content obtained from this study are however, lower than those reported for Cornelian Cherry (6.48%), Apricot Stone (7.18%,) and Almond Shells (7.21%), Sawdust (5.75%) and *Dalbergia sissoo* (6.24 %) [25].

According to Okieimen *et al* [26], the bulk density is an important physical parameter that is use to determine the amount of adsorbent that can be contained in a filter of given solid capacity and the amount of treated liquid that

can be retained by the filter cake. Higher density provides greater volume activity or lower porosity and normally indicates better quality adsorbent. The bulk densities obtained for RES and PESNP in this study were 0.687 g/cm^3 and 0.969 g/cm^3 respectively. These values were also higher than the bulk density reported for cornelian cherry and calcium oxide nanoparticles [19, 25].

The ash content of a sample is the inorganic residue left after the organic matter has been burnt off and it is a measure of the mineral content of the sample. Higher ash content values according to Getasew *et al* implies higher quality of the adsorbent for higher removal efficiencies [27]. The ash content of PESNP in this study was found to be higher than that of RES and also slightly higher when compared to results by other researchers [25, 27].

The pH of 1% solution of RES and PESNP were found to be 6.20 and 6.43 respectively which falls within the acceptable pH conditions. Most applications according to Okieimen *et al* generally accept pH of 6 – 8 [26].

3.1.2. Scanning electron microscopy (SEM) analysis

Scanning electron microscope (SEM) was used to take images of PESNP before and after treatment with methylene dye to determine the general look of particles such as shape. SEM micrograph of PESNP and dye treated PESNP are as presented in Figures 1 and 2 respectively.

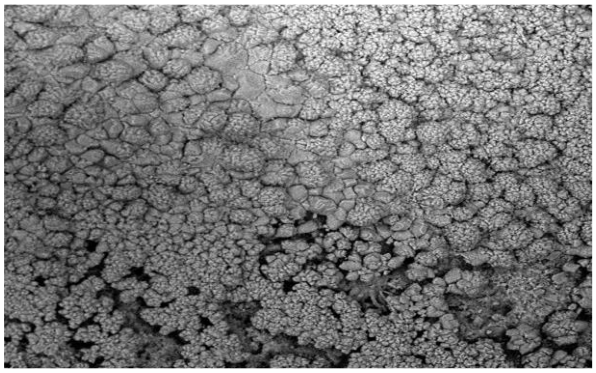

Figure 1. SEM image of Prepared Egg Shell Nano Particle

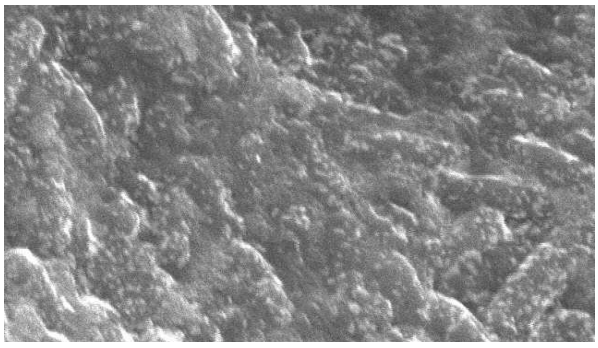

Figure 2. SEM image of dye treated Prepared Egg Shell Nano Particle

It can be observed from the image obtained for PESNP that its particles are of regular morphology and uniform in size. From Figure 2, it can be seen that there is a cluster arrangement that occurred after adsorption of the methylene dye onto PESNP which indicates that the dye molecules adhere to the surface of the PESNP. In other words we can say that the adsorbent surface was covered by complex formed by the dye molecules with PESNP. Similar observations have been reported by several other researchers [28 – 30].

3.1.3. X-ray fluorescence (XRF) Analysis

The X-ray fluorescence (XRF) analysis was carried out to provide information on the chemical composition of RES and PESNP and the data obtained is as listed in Table 2. It can be deduced from the results presented that $CaCO_3$ is the major compound in the raw eggshell (RES) amounting to about 88.03 % of the sample followed by CaO with 11.22%. However in the prepared egg shell nano particle (PESNP), CaO was found to be the major compound making up about 87.73 % of the sample followed by $CaCO_3$ with 10.24 % and the other oxide compounds amounts to only 2.03 % w/w. The high value of lime in PESNP indicated that the thermal treatment of eggshells during the calcination process to produce the nano particle transformed the chemical composition of the egg shell from calcium carbonate ($CaCO_3$) to calcium oxide (CaO) almost perfectly [20].

3.1.3. ***Thermal Degradation Analysis***

Thermal degradation analysis was carried out to provide information on both the heat flow and weight changes of PESNP as a function of temperature or time in a controlled atmosphere. The thermogram gotten from the thermo gravimetric analysis – differential Scanning Calorimetry (TGA – DSC) is as presented in Figure 3.

It can be deduced from the TGA – DSC curve that PESNP showed a two-step decomposition process. In the first decomposition step, a small heat flow of 21.8 mcal/sec adsorbed by the sample increased its temperature to 111 ^oC resulting to a minor weight loss of 11.5 % at 111 ^oC. This may be attributed to water desorption or dehydration [24]. The second decomposition is a thermal degradation which is as a result of the breakdown of $CaCO_3$ into CaO and release of carbon dioxide.

Table 2. The chemical composition of raw eggshell and prepared egg shell nanoparticle

S/N	CHEMICAL COMPOSITION	RAW EGG SHELL	SYNTHESIZED NANOPARTICLE
1	CaO	11.22	87.73
2	$CaCO_3$	88.03	10.24
3	Al_2O_3	0.03	0.04
4	MgO	0.31	0.72
5	SiO_2	0.01	0.08
6	Fe_2O_3	0.05	0.07
7	SO_3	0.06	0.09
8	K_2O	0.03	0.12
9	Na_2O	0.01	0.46
10	P_2O_5	0.25	0.45

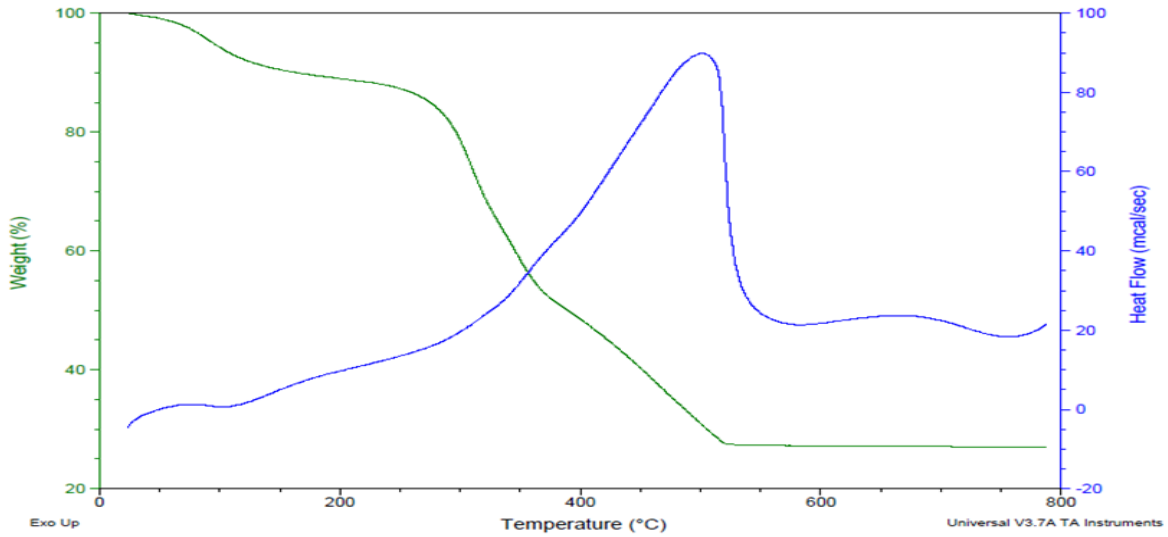

Figure 3. Thermogram of PESNP

3.2. Batch equilibrium studies

3.2.1. Effect of Initial dye ion Concentration

Table 3 presents data for the amount of equilibrium dye concentration by NPES from aqueous solutions containing various concentrations of the methylene blue dye at 298 K.

From the result, it can be seen that the adsorption capacity of PESNP increases with increase in the concentration of dye in solution. In other words, an increase in initial dye concentration leads to increase in the adsorption capacity of dye on PESNP. This indicated that initial dye concentrations played an important role in the adsorption of studied dye on the PESNP. It can also been seen that the uptake of the dye is favoured at the extremely low and high concentrations. This means that at low concentrations, adsorption sites of the adsorbent took up the available dye more rapidly or quickly; while at higher concentrations, the dye diffused to the adsorbent surface by intra particle diffusion [32 – 33]. Similar results were obtained for the adsorption of drim yellow-K4G on the shale oil ash and reactive blue 15 dye from an aqueous solution on cross-linked chitosan beads [33 - 34].

3.2.2. Effect of solution pH

The amount of methylene blue dye adsorbed from aqueous solutions by PESNP maintained at various pH is as presented in Table 4.

It can be deduced from the results that the removal efficiency of dye increased from 82.677 mg /g to 98.388 mg/g when the solution's pH was increased from 2 to 6. For pH values above 6, the adsorption capacity decreased with increase in pH. The mechanism of the studied dye adsorption by the adsorbent with pH variation could be explained with the same concept as put forward by Mall et al. [35] and Kumar [36], in that at lower pH more protons will be available to protonate the dye molecules. However these molecules become gradually deprotonated with increasing pH. Increase in degree of protonation will

usually lead to increasing degree of adsorption while increase in deprotonation will result in decrease in the degree of adsorption. The percentage removal of dye achieved in this study when the pH was varied were higher than those obtained by Arami [37] and Tsai et al [38] in their study of the removal of Direct Red 80 and Acid Blue 25 dyes from aqueous solutions on raw eggshell membrane respectively. This is expected as nanoparticles are expected to give better performance due to their higher surface area to its volume ratio.

3.2.3. Effect of contact time

Table 5 shows the variation of the amount of dye adsorbed by PESNP from aqueous solutions at various time intervals. From the results, it is indicative that the percentage removal of the dye increases with increase in contact time until equilibrium is reached at 80 mins. It was observed that process of adsorption was high at the initial stage and became slower while approaching the equilibrium stage. This is obvious due to the fact that more number of vacant charged sites available initially on the surface of the adsorbent and the sites are gradually filled up while approaching equilibrium and completely filled at equilibrium [30]. It is worthy to note that the percent dye removal only slightly increases with time. This could be attributed to an adsorption that is prevalent over desorption, a multi-layer adsorption or availability of more adsorption sites.

3.2.4. Effect of mass of adsorbent

Adsorption capacity of PESNP for methylene blue removal was also found to be influenced by mass of the adsorbent. Table 6 shows the amount of the studied dye adsorbed by various grams of PESNP at 303 K. From the results obtained, it can be seen that the more the biomass, the higher the removal efficiency. According to Ameh *et al* [39] and Zhang [40], increase in the efficiency of removal with an increase in the adsorbent dosage is due to the increase in the number of adsorbent binding sites. The phenomenon observed are similar to that reported in the adsorption of Acid Orange onto ground eggshell powder [38] and adsorption of Reactive Red 123 dye onto eggshell [41].

3.2.5. Effect of temperature

It has been reported that dye removal efficiency is dependent on temperature [42 – 43]. Table 7 presents equilibrium data on effect of temperature on adsorption the studied dye onto PESNP. It can be seen from the results presented that the extent of adsorption of the dye from aqueous solutions by PESNP decreased with increase in temperature and with modification. This indicates that the mechanism of adsorption of the dye onto PESNP is physical. For a physical adsorption mechanism, the extent of adsorption is expected to decrease with increase in temperature but for a chemisorption mechanism, the extent of adsorption is expected to increase with increase in temperature [42].

Table 3. Concentrations of dye adsorbed from aqueous solutions by PESNP containing various concentrations of the dye at 303 K

Concentration (mg/L)	**Amount of dye adsorbed** (mg/g)
10	63.278± 0.114
20	64.015 ± 0.221
40	64.881±0.194
60	64.962 ± 0.225
80	85.217 ± 0.472
100	96.765 ± 0.318

Table 4. Concentrations of dye adsorbed from aqueous solutions by PESNP and at various pH

pH	**Amount of dye adsorbed**
2	82.677± 1.938
4	95.698± 1.835
6	98.388± 1.999
8	90.989± 2.779
10	87.928± 3.717
12	79.021± 3.210

Table 5. Concentrations of dye adsorbed from aqueous solutions by PESNP at various time

t (min)	Amount of dye adsorbed
20	90.651± 1.133
40	95.454 ± 0.212
60	97.707 ±0.308
80	99.674 ±0.743
100	99.415 ±0.708

Table 6. Concentrations of dye adsorbed from aqueous solutions by PESNP and at various masses of adsorbent

M (g)	**Amount of dye adsorbed** (mg/g)
0.25	93.999± 0.146
0.50	99.999 ±0.110
1.00	99.862 ±0.041
2.00	99.844 ±0.081
3.00	99.840 ±0.080
5.00	99.800 ±0.090

Table 7. Concentrations of dye adsorbed from aqueous solutions by PESNP at various temperature

T (K)	Amount of dye adsorbed
303	99.676±0.172
323	98.878±0.614
333	97.758±0.061
343	97.585±0.019
353	96.312±0.613

3.3. Adsorption isotherm

In order to describe the equilibrium characteristics of adsorption, data obtained for the amount of the studied dye adsorbed per unit mass of the adsorbent at various concentrations from the study were fitted into different adsorption isotherms (Brunauer–Emmett–Teller, Langmuir, Freundlich, Redlich– Peterson, Temkin, Toth, Koble–Corrigan, Sips, Khan, Hill, Flory–Huggins and Radke–Prausnitz isotherm). From the results obtained, the best isotherms that described the adsorption characteristics of methylene blue dye on PESNP are Fruendlich and Temkin adsorption isotherms.

The expression establishing the Fruendlich adsorption isotherm can be written as follows [42].

$$q_e = K_F C_e^{\frac{1}{n}} \quad (12)$$

where q_e is the amount of adsorbate in the adsorbent at equilibrium (mg/g), K_F is the Fruendlich adsorption constant, n is related to the adsorption capacity and C_e is the equilibrium concentration of the adsorbate. The linear form of the Fruendlich isotherm is obtained by simplification of 12 which gives equation 13,

$$logq_e = logK_F + \frac{1}{n} logC_e \quad (13)$$

The Fruendlich isotherm was obtained by plotting $logq_e$ versus $logC_e$, giving a straight line (Figure 4). The Fruendlich isotherm constants n and K_F were determined from the slope and intercept of the plot ($logq_e$ versus $logC_e$), respectively. Table 8 present values of Fruendlich adsorption parameters deduced from the plots.

It can be seen that value of degree of linearity (R^2) is unity indicating the application of Freundlich adsorption model for the adsorption of methylene blue by PESNP. The suitability of this model isotherm to the adsorption of the studied dye onto PESNP implies that there is multilayer adsorption with non-uniform distribution over the heterogeneous surface [42]. The numerical value of n is a useful index to determine adsorption intensity or surface heterogeneity [4]

The values for n obtained in this study is higher than unity which according to Ruthven [44] suggests the existence of cooperative adsorption or follows mechanism of physical adsorption as against chemisorption mechanism (when n value is less than unity).

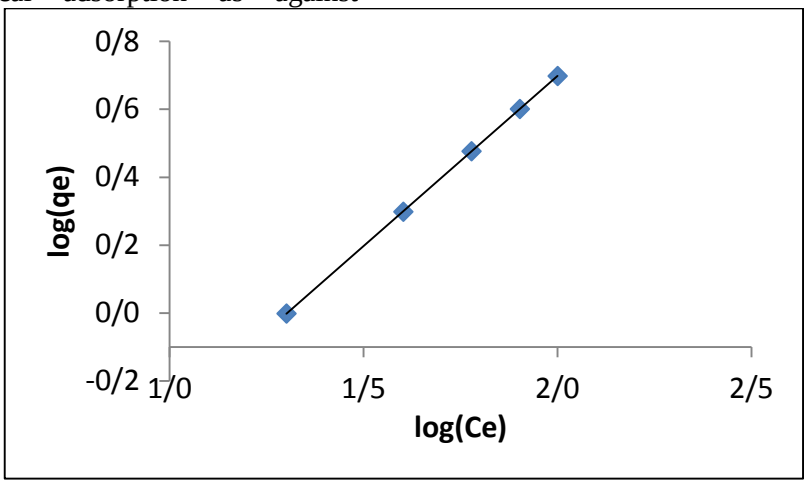

Figure 4. Variation of log(q_e) with log(C_e) for the adsorption of methylene blue onto PESNP

Table 8. Freundlich ,Temkin and Dubinin-Radushkevich parameters for the adsorption of methylene blue dye by PESNP

Freundlich Parameters				**Temkin Parameters**				**Dubinin-Radushkevich parameters**			
n	**logk_F**	**R^2**	ΔG^0_{ads} (kJ/mol)	**B**	**A**	**R^2**	ΔG^0_{ads} (kJ/mol)	a(mg^2/kJ^2)	ln(X_m)	E (kJ/mol)	R^2
0.1011	0.6101	1.0000	-17.66	26.15	31.55	0.9551	-22.66	0.68	1752.1	1.0813	0.9764

The adsorption of methylene blue onto PESNP was also found to obeyed the Temkin adsorption model, which it linearized form is given by equation 14 [42] .

$$q_e = \frac{RT}{B} lnA + \frac{RT}{B} lnC_e \quad (14)$$

where q_e is the amount of adsorbate in the adsorbent at equilibrium, R is the gas constant, T is the temperature, B is the Temkin isotherm constant, A is the Temkin isotherm equilibrium binding constant and C_e is the equilibrium concentration

From equation 14, a plot of q_e versus lnC_e should be linear with slope and intercept equal to $\frac{RT}{B}$ and $\frac{RT}{B}$ lnA respectively. Figure 5 show the Temkin isotherm for the adsorption of methylene blue by PESNP.

The Temkin adsorption parameters derived from the plot are also recorded in Table 8. R^2 value calculated from the plot was very close to unity indicating that the application of the Temkin isotherm for the adsorption of the dye by PESNP. The value of the Temkin isotherm constant (B) obtained was positive and relatively low indicating the attractive behavior of the adsorbent. Generally, the higher the value of B, the higher the degree of interaction between the adsorbate and the adsorbent. The present data strongly point toward a relatively weak interaction, which also supports the mechanism of physical adsorption.

The Fruendlich adsorption constant (K_F) and Temkin equilibrium constant (A) were used to estimate the free energy of adsorption of the studied dye using equation 15 and 16 respectively [39],

$$\Delta G^0_{ads} = -2.303RTlogK_F \quad (15)$$

$$\Delta G^0_{ads} = -2.303RTlogA \quad (16)$$

Values of ΔG^0_{ads} calculated from equations 15 and 16 are also recorded in Table 8. From the results obtained, the free energies are negatively less than the threshold value expected for the mechanism of chemical adsorption, which also suggest that the adsorption of the studied dye onto PESNP is physical.

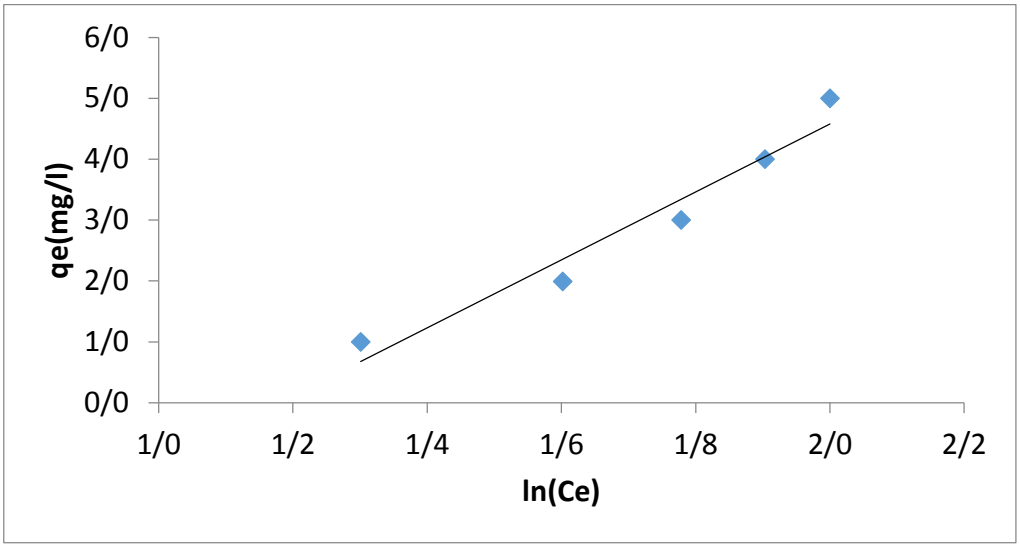

Figure 5. Variation of q_e with $\ln(C_e)$ for the adsorption of methylene blue onto PESNP

Dubinin-Radushkevich (D-RIM) adsorption isotherm was applied to predict/confirm the mechanism of adsorption of the studied dye onto PESNP. The Dubinin-Radushkevich (D-RIM) adsorption isotherm can be expressed according to equation 17 [45].

$$lnq_e = lnX_m - a\delta^2 \quad (17)$$

where q_e (mgl/g) is the concentration of the adsorbate adsorbed in the adsorbent, X_m (mg/g) is the maximum sorption capacity, "a" can be defined as half the square of the reciprocal of the mean adsorption energy (i.e. a = ½ (1/ ε)^2. and δ is the polany potential which can be estimated from the equation 18,

$$\delta = RTln\left(1 + \frac{1}{C}\right) \quad (18)$$

From equation 18, a plot of lnq_e versus δ^2 should give a straight line with slope equals to a constant, 'a'. It has been found that ε value less than 8 kJ/mol supports the mechanism of physical adsorption but ε values greater than 8 kJ/mol are consistent with the mechanism of chemisorption.

Figure 6 shows D-RIM isotherm for the adsorption of dye onto PESNP. Adsorption parameters obtained together with the correlation coefficient from the plot is as presented in Table 8 and it further indicated that the mechanism of adsorption was consistent with physical adsorption.

3.4. Adsorption kinetics

The pseudo first order and pseudo second order kinetic models were used to investigate the mechanism of adsorption and potential rate controlling step involved in the adsorption of the dye onto PESNP.

The pseudo first order equation is given as below [30]:

$$\log(q_e - q_t) = \log(q_e) - \left(\frac{k_1}{2.303}\right)t \quad (19)$$

where q_e and q_t are the amount of heavy metal ions adsorbed at equilibrium and at time, t (respectively mg/g) and k_1 is the first order rate constant (min^{-1}).

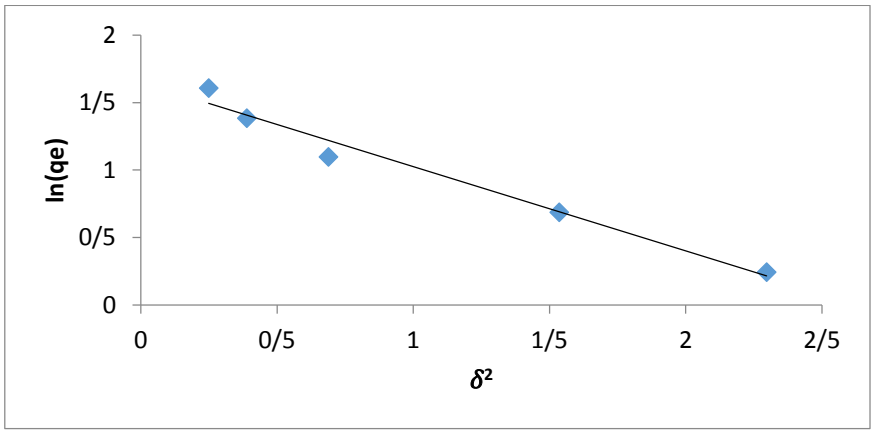

Figure 6. Variation of $\ln(q_e)$ with δ for the adsorption of methylene blue onto PESNP

From equation 19, a plot of $\log(q_e - q_t)$ versus t is expected to be linear if the Lagergren model is obeyed with slope and intercept equal to $k_1/2.303$ and $\log(q_e)$ respectively.

The linearized pseudo second-order kinetic model is expressed as shown in equation 20 [30]

$$\frac{t}{q_e} = \left(\frac{1}{k_2 q_e^2}\right) + \left(\frac{1}{q_e}\right)t \qquad (20)$$

where k_2 is the second order rate constant. The implication of equation 20 is that a plot of $\frac{t}{q_e}$ versus t should be a straight line with slope and intercept equal to $\frac{1}{q_e}$ *and* $\frac{1}{k_2 q_e^2}$ respectively. Figures 7 and 8 show kinetic plots for pseudo first order and pseudo second order model respectively. Kinetic constants calculated from the slope and intercept of the plots are presented in Table 9.

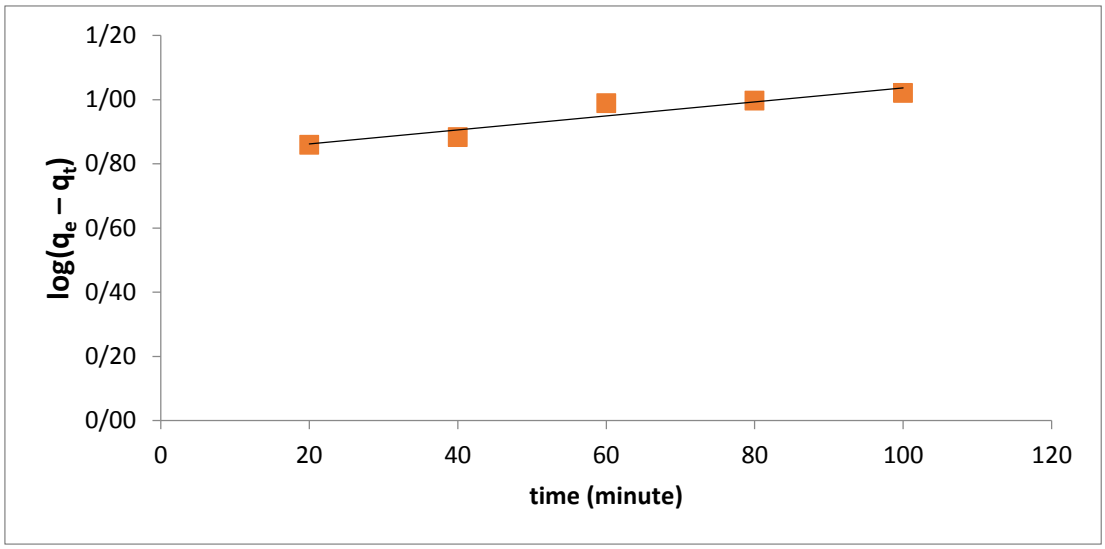

Figure 7. Variation of $\log(q_e - q_t)$ with t for the adsorption of methylene blue onto PESNP

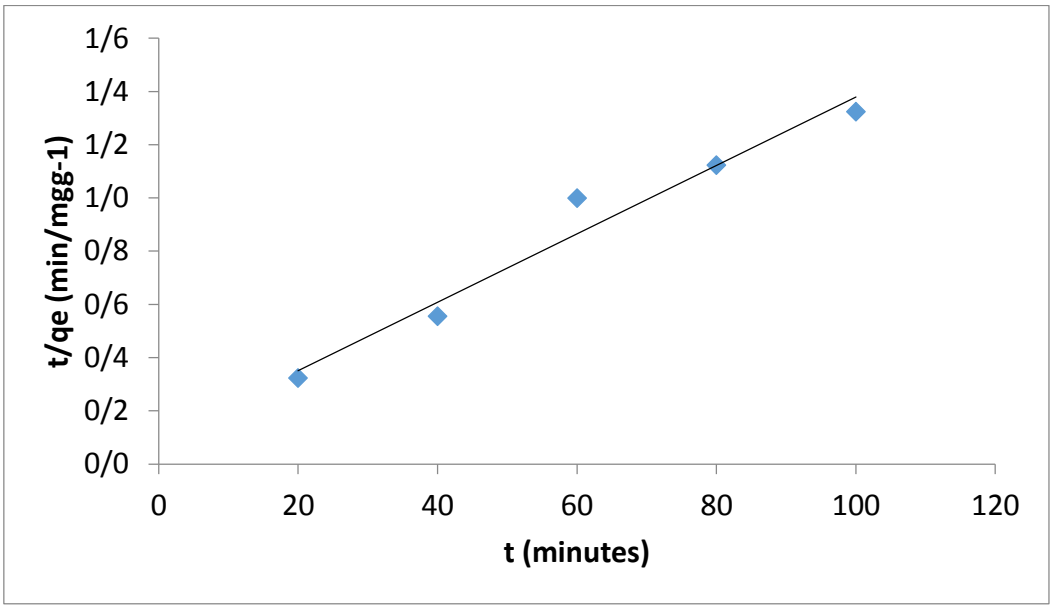

Figure 8. Variation of $\frac{t}{q_e}$ with t for the adsorption of methylene blue onto PESNP

Table 9. Pseudo first and second order rate constants for the adsorption of methylene blue dye by PESNP

q_e (mg/g)	k_1 (min^{-1})	R^2	q_e (mg/g)	K_2 ($gmg^{-1}min^{-1}$)	R^2
1.0156	0.0061	0.8904	79.1347	0.0003	0.9644

It can be deduced that correlation coefficients (R^2) values for the pseudo second order adsorption model was higher (0.9644) and closer to unity than that of pseudo first order adsorption model (0.8904) indicating that the adsorption of methylene blue dye onto PESNP is consistent with a Pseudo second order kinetics.

3.5. Quantum Chemistry study

The values of some quantum chemical parameters calculated for the studied dye molecule is as presented in Table 10. The frontier molecular orbital energies (energy of the highest occupied molecular orbital, E_{HOMO}, and that of the lowest unoccupied molecular orbital, E_{LUOMO}) are important parameters for defining the reactivity of a chemical species. Therefore, an increase in the value of E_{HOMO} is associated with increasing ease of adsorption. On the other hand, E_{LUMO} indicates the ability of a molecule to accept electrons, which implies the lower the value of E_{LUMO} better should be the adsorption potential [46]. Larger values of the energy gap (ΔE) imply low reactivity to a chemical species. The total Potential Energy, electronic energy, binding energy, hydration energy of the molecule are all essential parameters that have been proven to be associated with adsorption ability of a compound. Generally, the lower the values of these energies, the higher the ease or tendency of the molecule to be adsorbed onto a surface. These parameters also within the range of values expected for some molecules that can easily adhere to adsorbents [46]. Figures 9 showed the distribution of HOMO and LUMO of the studied dye molecule. From the figures presented, it could be seen that the distribution of HOMO is mainly located at chlorine atoms while the LUMO orbital distributions are mainly localized around the benzene ring, nitrogen and sulphur atoms. This kind of distribution favoured parallel adsorption of the methylene dye onto the adsorbent surface via two modes. One mode is that the dye molecules donate electrons to unoccupied orbitals of adsorbent atoms forming coordinate bond and the other mode is that the dye molecules accept electrons from the atoms in the adsorbent to form back-donating bond.

The local selectivity of an inhibitor can be analyzed using condensed Fukui and condensed softness functions**.** According to Udhayakala [47]**,** fukui functions compute local reactivity indices that makes possible to rationalize the reactivity of individual molecular orbital contributions. The condensed Fukui function and local softness indices allow one distinguish each part of the molecule on the basis of its distinct chemical behaviour due to the different substituted functional group. It has been reported that the preferred site for electrophilic attack is the place where the value of f_k^- is maximum while the site for nucleophilic attack is the atom in the molecule where the value of f_k^+ is maximum [47]. The calculated Fukui function for the studied dye is presented in Tables 11. It can be deduced from the results presented that the active sites for nucleophilic attack

Table 10. Quantum chemical parameters of methylene blue dye

PARAMETER	VALUE
E_{HOMO}(eV)	-6.573
E_{LUMO}(eV)	-2.676
ΔE(eV)	3.897
IP	6.573
EA	2.676
Ƞ (ev)	1.9485
δ (ev)	0.5131
χ (ev)	-4.625
ω (ev)	5.488
N (ev)	6.941
Total Potential Energy (Kcal/mol)	-138398.68
Electronic Energy of Molecule (Kcal/mol)	-179980.30
Binding energy of molecule (Kcal/mol)	-4945.93
Hydration energy (Kcal/mol)	−7.1500

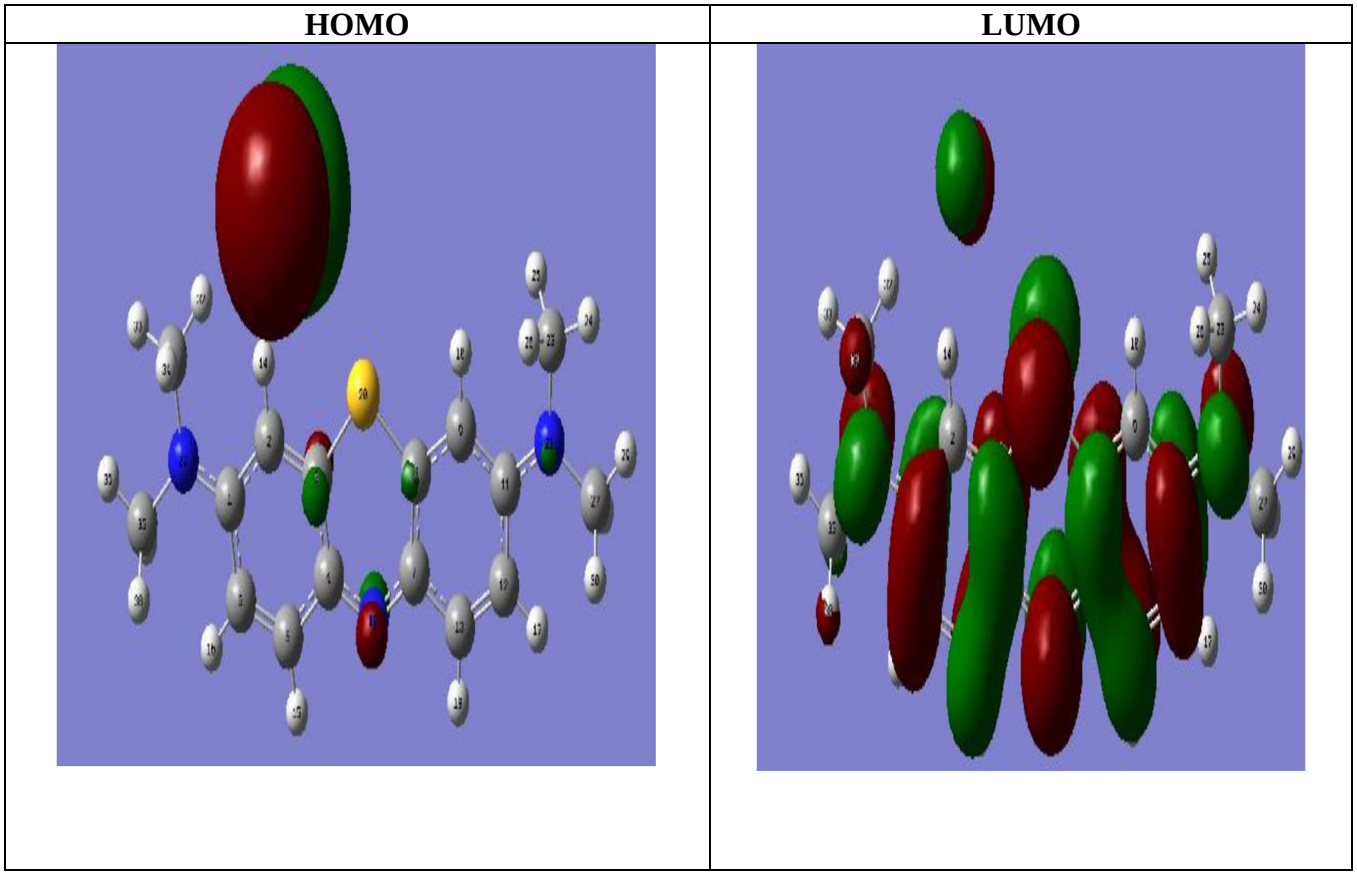

Figure 9. Frontier Molecular Orbitals and electronic distribution for Methylene blue

in the molecule may be located at N (19) and S (20) atoms of the methylene dye while the site for electrophilic attack is mainly located in the aromatic ring at C (2) , C (3) and Cl (39). The molecular orbital diagram as presented in Figure 9 (green represents positive and maroon represents negative) clearly support the findings derived from the Fukui calculations. This may be explained as follows: the HOMO is related to the electrophilic Fukui function (fk^{+}) while the LUMO is related to the nucleophilic Fukui function (fk^{-}). Thus, it could be concluded that these atoms with high fk^{+} and fk^{-} would have strong interaction with the adsorbent surface via exchanging electrons.

Table 11. Fukui and softness functions for electrophilic and nucleophilic attacks on carbon and electronegative atoms in the studied dye

Atom No	f_x^+	f_x^-
C(1)	0.11125	0.027367
C(2)	-0.06521	**0.15551**
C(3)	0.11356	**0.17121**
C(4)	-0.04662	0.13340
C(5)	0.13121	0.10415
C(6)	-0.06451	-0.01521
C(7)	-0.0674	0.08424
C(8)	0.14851	-0.00378
C(9)	0.03401	-0.00381
C(10)	0.12733	-0.00123
C(11)	0.11431	-0.00467
C(12)	0.10722	-0.00411
C(13)	0.12144	-0.00184
C(14)	-0.55310	-0.00511
C(16)	-0.00141	-0.00268

C(17)	-0.45621	-0.01251
N(19)	**0.61441**	-0.10232
S(20)	**0.72996**	-0.11832
N(21)	0.04758	0.08943
N(22)	0.06775	0.17020
Cl(39)	0.02911	**0.65461**

4. Conclusion

The results and findings of this study reveal that nano particles prepared from waste eggshell can effectively remove hazardous dyes like methylene blue from wastewater, which may alleviate the environmental impact of dyeing industries. The percentage of dye removed by PESNP depends on the variation of adsorbent dosage, initial dye concentration, solution pH, temperature and contact time. The equilibrium adsorption data obtained at different concentrations fitted well with Freundlich, and Temkin adsorption isotherm. Adsorption parameters deduced from these isotherm indicated the presence of strong interaction between the adsorbate and the adsorbent and the existent of the mechanism of physical adsorption. Pseudo-second-order equation was better in describing the adsorption kinetics of the methylene blue on PESNP. Computational chemistry can be adequately be used to predict the direction of the adsorption process.

Acknowledgements

The research work that generated this publication was fully sponsored by the Tertiary Education Trust Fund of Nigeria (TETFUND) through the National Research grant with Dr. Ameh Paul Ocheje as the Principal investigator

References

[1] H. E. Gall, O. Mina, "Coping with emerging contaminants in potable water sources," Handbook of Environmental Chemistry, 30 (2014) 61 – 93.

[2] S. A. Parsons, B. Jefferson, Organic Removal, Introduction to Potable Water Treatment Processes-John Wiley and Sons. (2006) 66 – 68.

[3] A. El Nemr, O. Abdelwahab, A. El-Sikaily, A. Khalde, Removal of direct blue-86 from aqueous solution by new activated carbon developed from orange peel. *Journal of Hazardous Mate*rial, 161 (2009) 102–110.

[4] P. O. Ameh. Adsorption of nickel (II), cadmium (II) and lead (II) from aqueous solution using chitosan / raphia palm composite, *Algerian Journal of Material Chemistry*, 3(2) (2020) 48–60.

[5] A. N. A El-Hendawy, S.E Samara, B.S Giris. Adsorption characteristics of activated carbons obtained from corncorbs. *Colloids and Surf. A: Physicochemical and Engineering Aspects*, 180 (2001) 209-221.

[6] S. Nethaji, A. Sivasamy, Removal of hexavalent chromium from aqueous solution using activated carbon prepared from walnut shell biomass through alkali impregnation processes. *Clean Technologies and. Environmental Policy*, 16(2) (2014) 361 – 368.

[7] I. Enniya , L. Rghioui , A. Jourani , Adsorption of hexavalent chromium in aqueous solution on activated carbon prepared from apple peels. *Sustainable. Chemistry and Pharmacy*, 7 (2018) 9-16.

[8] M. K Rai, B. S Giri, Y. Nath , H. Bajaj, S. Soni , R.P Singh, R. S Singh, B. N. Rai , Adsorption of hexavalent chromium from aqueous solution by activated carbon prepared from almond shell: kinetics, equilibrium and thermodynamics study. *Journal of Water Supply: Research and Technology.-Aqua*. 67(8) (2018) 724-737.

[9] R. Labied, O. Benturki, A.Y Eddine, A. Donnot, Adsorption of hexavalent chromium by activated carbon obtained from a waste lignocellulosic material (Ziziphus jujuba cores): Kinetic, equilibrium, and thermodynamic study, *Adsorption Science and Technology*, 36(3-4) (2018) 1066-1099.

[10] P .O. Ameh. Modelling of the Adsorption of Cu (II) and Cd (II) from Aqueous Solution by Iraqi Palm-Date Activated Carbon (IPDAC) *International Journal of Modern Chemistry*, 5(3) (2013) 136-144.

[11] A. Mullick , S Moulik , S. Bhattacharjee , Removal of hexavalent chromium from aqueous solutions by low-cost rice husk-based activated carbon: kinetic and thermodynamic studies. *Indian Chemical Engineer*, 60(1) (2018) 58-71.

[12] S. H Azaman, A. Afandi , B.H Hameed , A.M Din, Removal of malachite green from aqueous phase using coconut shell activated carbon: Adsorption, desorption, and reusability studies. *Journal of Applied Science. And Engineering*, 21(3) (2018) 317-330.

[13] M. Razavi Mehr, M. H Fekri, F. Omidali, N. Eftekhari, B. Akbari-adergani, Removal of chromium (VI) from wastewater by palm kernel shell-based on a green method. *Journal of Chemical Health Risks*, 9(1) (2019) 75-86.

[14] T. Dula, K. Siraj, S. A Kitte. Adsorption of hexavalent chromium from aqueous solution using chemically activated carbon prepared from locally available waste of bamboo (Oxytenanthera abyssinica). *International Scholarly Research Notices*, (2014) 1-14.

[15] V. E Pakade, O. B Nchoe, L. Hlungwane, N. T Tavengwa. Sequestration of hexavalent chromium from aqueous solutions by activated carbon derived from Macadamia nutshells. *Water Science and. Technology*, 75(1) (2017) 196-206.

[16] S. Bhattacharya, I Saha, A. Mukhopadhyay, D. Chattopadhyay, UC Ghosh, Role of nanotechnology in water treatment and purification: Potential applications and implications. *International Journal of Chemical Science and Technology*, 3 (2013) 59-64.

[17] K. Kumaraswamy, B. V. Dhananjaneyulu,, P. Vijetha, Y. Kumar, Kinetic and equi- librium studies for the removal of chromium using eggshell powder. *Research Journal of Pharmaceutical, Biological and. Chem*ical Sciences, (2015) 529–532.

[18] R. G. Jalu, , A. T. Chamada , R. Kasirajan , Calcium oxide nanoparticles synthesis from hen eggshells for removal of lead (Pb(II)) from aqueous solution, *Environmental Challenges*, 4 (2021) 100193.

[19] N. Tangboriboon, R. Kunanuruksapong, A. Sirivat, Preparation and properties of calcium oxide from eggshells via calcination, *Materials. Science. -Poland*, 30(4) (2012) 313-322.

[20] A. Aziza, A. Odiakosa, G. Nwajei, V. Orodu, V, Modification and Characterization of Activated Carbon derived from Bumper Sawdust and Sawdust to remove Lead(II) and Cadmium(II) Effluent Water. *CSN Conference Proceeding. Chemical Society of Nigeria*, (2008) 235-243.

[21] AOAC. "Association of official Analytical Chemists. Official Methods of Analysis" 15th Edn. Washing D.C, USA (1990) 69-88.

[22] J. C. Igwe, A. A. Abia, Adsorption kinetics and intraparticulate diffusivities for bioremediation of Co (II), Fe (II) and Cu (II) ions from waste water using modified and unmodified maize cob. *International Journal of Physical Science,s* 2(5) (2007) 119-127.

[23] P. O. Ameh, N. O. Eddy. Theoretical and Experimental Investigations of the Corrosion Inhibition Action of *Piliostigma Thonningii* Extract on Mild Steel in Acidic Medium. *Communication in Physical Sciences*, 3(2) (2018) 27-42.

[24] C. E. Gimba, Preparation and Adsorption Characteristics of Activated Carbon From Coconut Shell. Ph.D Thesis, Ahmadu Bello University, Zaria Nigeria . (2001).

[25] F. E. Okieimen, F. I Ojokoh, C. O. Okieimen, R. A. Wuana, Preparation and Evaluation of activated carbon from Rice husk and rubber seed shell. *Chemical Class Journal*, (2004) 191 – 196.

[26] Z. A. Getasew Ketsela, T. Alemu, Adsorption of lead (II), Cobalt (II) and Iron (II) from aqueous solution by activated carbon prepared from white lupine (GIBITO) HSUK. *Journal of Thermal Analysis and. Calorimetry*, (2020) 2157–7544.

[27] A. M. Salvador, J. A. Pellicer, M. I. Rodríguez-López, V. M. Gómez-López , E. Núñez-Delicado and J. A. Gabaldón, Egg By-Products as a Tool to Remove Direct Blue 78 Dye from Wastewater: Kinetic, Equilibrium Modeling, Thermodynamics and Desorption Properties, *Materials*, 13, (2020) 1–18 .

[28] U. Yunusa , U. Bishir, M. B. Ibrahim , Kinetic and thermodynamic studies of malachite green adsorption using activated carbon prepared from desert date seed shell. *Algerian Journal of Engineering and Technol*ology 2 (2020) 37-45.

[29] V. K. Gupta, A. Rastogi,. Biosorption of lead from aqueous solutions by green algae *spirogyra species*. Kinetics and equilibrum studies. *Journal of Colloid and Interface Science.*, 296 (2007) 59 – 63.

[30] W.T. Tsai, C. Y. Chang, C. F. Wang, S. F Chien. H. F Sun, Preparation of Activated Carbons from Carbon corn cob catalyzed by potassium salts and subsequent gasification with CO_2. *Bioresource. Technology* 78 (2) (2001) 203-208.

[31] M. S. Chiou, G. S. Chuang, Competitive adsorption of dye metanil yellow and RB15 in acid solutions on chemically cross-linked chitosan beads, *Chemosphere* 62 (2006) 731–740.

[32] M. S. Chiou, H. Y. Li, Adsorption behavior of reactive dye in aqueous solution on chemical cross-linked chitosan beads, *Chemosphere* 50 (2003) 1095–1105.

[33] Z. Al-Qoda, Adsorption of dyes using shale oil ash, *Water Research*. 34 (2000) 4295–4303

[34] I. D Mall, V. C Srivastava, N. K. Agarwal,. Adsorptive removal of malachite green dye from aqueous solution by bagasse fly ash and activated carbon- kinetic study and equilibrium isotherm analyses. *Colloids and Surf. A: Physicochemical and Engineering Aspects*, 264(1–3) 2005:17–28.

[35] M. N. V. Ravi Kumar, A review of chitin and chitosan applications, *Reactive and Functional. Polymers*, 46 (2000) 1–27.

[36] M. Arami,. , N. Y Limaee. N. M Mahmoodi,. Investigation on the adsorption capability of egg shell membrane towards model textile dyes, *Chemosphere* 65 (2006), 1999–2008

[37] W. T. Tsai,. K. J. Hsien,. H. C. Hsu,. C. M. Lin, K. Y. Lin, C. H Chiu,. Utilization of ground eggshell waste as an adsorbent for the removal of dyes from aqueous solution. *Bioresource Technol*ogy, 99 (2008) 1623–1629.

[38] P. O Ameh, R. Odoh, A Oluwaseye, . Equilibrium Study on the Adsorption of Zn(II) and Pb (II) ions from Aqueous Solution onto *Vitex doniana* Nut *International. Journal of Modern Chemistry*, 3(2) (2012) 82-97.

[39] H. Zhang, L Liu. , J. Liu. , L Hongping, J Liu. ,. Equilibrium, kinetics and thermodynamics studies of Lead (II) biosorption on Semame husks. *Bioresource*, 7(3) (2012) 3555–3572.

[40] M. Ehrampoush, G. Ghanizadeh, M. Ghaneian, Equilibrium and kinetics study of reactive red 123 dye removal from aqueous solution by adsorption on eggshell. *Journal of Environmental Health Science and Engineering*, 8 (2011) 101–106.

[41] A. W. Adamson, A. P. Gast, Physical Chemistry of Surfaces, sixth ed., Wiley- Interscience, New York (1997).

[42] E. Demirbas, M. Kobya, A.E.S. Konukman, Error analysis of equilibrium studies for the almond shell activated carbon adsorption of Cr(VI) from aqueous solutions, *Journal of Hazardous Mateials*. 154 (2008) 787–794.

[43] D. M. Ruthven, Principles of Adsorption and Adsorption Processes, Wiley, New York, (1984).

[44] M. Y. Chang, R. S. Juang, Adsorption of tannic acid, humic acid, and dyes from water using the composite of chitosan and activated clay, *Journal of Colloid and Interface Science*, 278 (2004) 18–25.

[45] P.O Ameh, N.O Eddy, Theoretical and experimental studies on the corrosion inhibition potentials of 3-nitrobenzoic acid for mild steel in 0.1 M H_2SO_4. *Cogent Chem*. 2 (2016) 1 – 12 .

[46] P. Udhayakala. Quantum chemical studies on the inhibition potentials of thiophene derivatives for the corrosion inhibitors of carbon steel, *Journal of Chemical and Pharmaceutical Research*, 7(1) (2015) 803-810